Atmospheric
Measurement
Techniques

Implementation of electrochemical, optical and denuder-based sensors and sampling techniques on UAV for volcanic gas measurements: examples from Masaya, Turrialba and Stromboli volcanoes

Julian Rüdiger[1,a], Jan-Lukas Tirpitz[2], J. Maarten de Moor[3], Nicole Bobrowski[2,4,5], Alexandra Gutmann[1], Marco Liuzzo[6], Martha Ibarra[7], and Thorsten Hoffmann[1]

[1]Johannes Gutenberg-University, Institute of Inorganic and Analytical Chemistry, Mainz, Germany
[2]University of Heidelberg, Institute for Environmental Physics, Heidelberg, Germany
[3]Observatorio Vulcanológico y Sismológico de Costa Rica, Heredia, Costa Rica
[4]Johannes Gutenberg-University, Institute of Geosciences, Mainz, Germany
[5]Max Planck Institute for Chemistry, Mainz, Germany
[6]Istituto Nazionale di Geofisica e Vulcanologia, Sezione di Palermo, Italy
[7]Instituto Nicaragüense de Estudios Territoriales, Managua, Nicaragua
[a]now at: University of Bayreuth, Atmospheric Chemistry, Bayreuth, Germany

Correspondence: Julian Rüdiger (j.ruediger@uni-mainz.de) and Thorsten Hoffmann (hoffmant@uni-mainz.de)

Abstract. Volcanoes are a natural source of several reactive gases (e.g., sulfur and halogen containing species) and non-reactive gases (e.g., carbon dioxide) to the atmosphere. The relative abundance of carbon and sulfur in volcanic gas as well as the total sulfur dioxide emission rate from a volcanic vent are established parameters in current volcano-monitoring strategies, and they oftentimes allow insights into subsurface processes. However, chemical reactions involving halogens are thought to have local to regional impact on the atmospheric chemistry around passively degassing volcanoes. In this study we demonstrate the successful deployment of a multirotor UAV (quadcopter) system with custom-made lightweight payloads for the compositional analysis and gas flux estimation of volcanic plumes. The various applications and their potential are presented and discussed in example studies at three volcanoes encompassing flight heights of 450 to 3300 m and various states of volcanic activity. Field applications were performed at Stromboli volcano (Italy), Turrialba volcano (Costa Rica) and Masaya volcano (Nicaragua). Two in situ gas-measuring systems adapted for autonomous airborne measurements, based on electrochemical and optical detection principles, as well as an airborne sampling unit, are introduced. We show volcanic gas composition results including abundances of CO_2, SO_2 and halogen species. The new instrumental setups were compared with established instruments during ground-based measurements at Masaya volcano, which resulted in CO_2 / SO_2 ratios of 3.6 ± 0.4. For total SO_2 flux estimations a small differential optical absorption spectroscopy (DOAS) system measured SO_2 column amounts on transversal flights below the plume at Turrialba volcano, giving $1776 \pm 1108\,\mathrm{T\,d^{-1}}$ and $1616 \pm 1007\,\mathrm{T\,d^{-1}}$ of SO_2 during two traverses. At Stromboli volcano, elevated CO_2 / SO_2 ratios were observed at spatial and temporal proximity to explosions by airborne in situ measurements. Reactive bromine to sulfur ratios of 0.19×10^{-4} to 9.8×10^{-4} were measured in situ in the plume of Stromboli volcano, downwind of the vent.

1   Introduction

Gaseous volcanic emissions consist of a variety of different compounds and are dominated by water vapor (H_2O), carbon dioxide (CO_2), sulfur dioxide (SO_2), and hydrogen sulfide (H_2S) (Symonds et al., 1994). Minor abundant but nonetheless important gas species are halogen-bearing compounds which are emitted as hydrogen halides (HF, HCl, HBr and HI) and later partly transformed by heterogeneous reactions into other halogen species, such as bromine monoxide (BrO) or chlorine dioxide (OClO) (Bobrowski et al., 2007). The relative gas composition varies with the types of volcanoes and magmas as well as with transport and degassing mechanisms. Changes in the magma degassing behavior and/or the hydrothermal systems beneath volcanoes generally influence the gas composition and gas fluxes. Measuring the emitted gas composition can provide crucial information on understanding subsurface processes related to activity changes (e.g., Allard et al., 1991; Aiuppa et al., 2007; Bobrowski and Giuffrida, 2012; de Moor et al., 2016a; Liotta et al., 2017) and help to estimate fluxes of the geological carbon cycle (e.g., Burton et al., 2013; Mason et al., 2017) and tectonic processes controlling volcanic degassing (e.g., Aiuppa et al., 2017; de Moor et al. 2017). In the field of volcanic monitoring, the observation of gas composition changes has become an important tool for detecting precursory processes for volcanic eruptions. For instance, the CO_2 / SO_2 emission ratio strongly varies with volcanic activity, which is associated with magma rising up a conduit. The solubility of magmatic gases is pressure dependent and different gases are released from the magma at different depths during the magma ascent, which is accompanied by a pressure decrease. Gas ratio changes have been observed within timescales of hours to weeks prior to eruptions (e.g., Giggenbach, 1975; Aiuppa et al., 2007; de Moor et al., 2016a, de Moor et al., 2016b) and their magnitude, direction, and pace are highly variable throughout different volcanic systems and states of activity. In situ measurements of this gas ratio have become well-established in usage of electrochemical (SO_2) and infrared (CO_2) sensors, which are implemented in Multi-GAS (MG) instruments. These instruments may also contain other sensors and are field deployable, meaning they are autonomous and can work close to volcanic emission sources (Shinohara, 2005; Aiuppa et al., 2006). Another important parameter for the characterization of volcanic activity is the gas emission rate. In particular, the determination of SO_2 flux has become a standard procedure. It involves traversing the plume and multiplying the integrated SO_2 cross section with the estimated plume transport speed (e.g., McGonigle et al., 2002; Galle et al., 2003; López et al., 2013). With the development of small DOAS instruments, traversing the plume is not only feasible by car, boats, or manned aircraft, but also by walking, in the case of poorly accessible terrain. Furthermore, knowledge about in-plume chemical reactions can be drawn from compositional assessment of the gases, which

also helps to understand their impact on atmospheric chemistry (e.g., Lee et al., 2005; von Glasow et al., 2009; von Glasow, 2010; Gliß et al., 2015). The halogen chemistry is of especially great interest as BrO / SO_2 ratios in volcanic plumes are readily measurable by remote sensing UV spectrometry (e.g., Bobrowski et al., 2003; Lübcke et al., 2014) and have been discussed in recent years as another potential precursory observable parameter for volcanic activity changes. Although several studies observed decreases in the BrO / SO_2 ratio before eruptive phases (e.g., Lübcke et al., 2014) and lower ratios during periods of continuous activity (Bobrowski and Giuffrida, 2012), it is not yet clear whether magma–gas partitioning of bromine occurs before or after sulfur during the pressure drop associated with magma ascents (Dinger et al., 2018). Furthermore, BrO is not a directly emitted species; rather it is the product of complex heterogeneous chemistry in the volcanic plume involving reactions with magmatic gases with entrained air (e.g., Gerlach, 2004; Bobrowski et al., 2007). Differential optical absorption spectroscopy (DOAS) measurements revealed a variation in BrO concentration with plume age and transversal position inside the plume (Bobrowski et al., 2007). Additionally, other reactive halogen species with oxidation states $\neq -1$ (e.g., Br_2, Cl_2, BrCl and others) have been measured in situ in the plume of Mt. Etna, Italy (Rüdiger et al., 2017) and Mt. Nyamuragira (Bobrowski et al., 2017). In the last decade, several model studies (e.g., Bobrowski et al., 2007; Roberts et al., 2009; von Glasow, 2010; Roberts et al., 2014; Jourdain et al., 2016) have engaged with the variation in halogen variability in volcanic plumes with respect to various atmospheric and magmatic parameters. In the case of bromine, it was modeled that the initial emitted hydrogen bromide is depleted shortly after emission under consumption of tropospheric ozone and is transformed to reactive species such as BrO, HOBr, Br_2, BrCl and $BrONO_2$. Due to the challenging task of accessing volcanic plumes on a timescale of minutes after emission and the lack of spectroscopic methods for most of these reactive species, uncertainties about their relative abundances still exist. One approach to the in situ observation of reactive halogen species is the application of gas diffusion denuder sampling using a selectively reactive organic coating (1,3,5-trimethoxybenzene, TMB) to trap and enrich gaseous species containing a halogen atom with the oxidations state $+1$ or 0 (e.g., Br_2 or BrCl), while being insensitive to the particle phase (Rüdiger et al., 2017).

In the case of most volcanoes, sampling on the crater rim may be associated with considerable logistical challenges and hazards for people and instruments. During phases of high activity crater rims are usually not accessible at all and, even during quiescent degassing, work at the crater rim represents a considerable risk. However, the knowledge of plume gas composition is an important component for activity assessments of volcanoes (e.g., Carroll and Holloway, 1994; Aiuppa et al., 2006) and therefore gas monitoring stations are deployed and maintained in close proximity to active vol-

canic vents by researchers, putting themselves at risks. Advancements in the application of remote sensing techniques have helped to minimize personnel exposition to the volcanic danger zone (e.g., Galle et al., 2003; Tamburello et al., 2011). However, still today the detection of certain gas species and/or total amounts of all species of an element is not possible remotely (neither ground based nor with satellites) and therefore in situ measurements are an important tool, especially for resolving chemical reactions and speciation changes in aging volcanic plumes. With an in situ sampling strategy, obtaining samples from the freshly emitted plume is feasible, while ground-based in situ sampling of the aged plume further downwind is rarely possible and is dependent on specific wind and geographical conditions. In the last decade, with the development of compact and cost effective unmanned aerial vehicles (UAV), several deployments of gas sensors and other in situ methods, e.g., particle detection (Altstädter et al., 2015), as well as applications of spectrometers were realized (e.g., McGonigle et al., 2008; Diaz et al., 2015; Mori et al., 2016; Villa et al., 2016 and references therein). Pioneering UAV deployments were already conducted in the late 1970s (Faivre-Pierret et al., 1980). While these drone-based applications focused mostly on the use of sensors and spectroscopy methods, here we present a low-cost UAV-deployable sampling (gas diffusion denuder) and sensing (electrochemical/optical sensors) systems for the determination of CO_2, SO_2 and halogen species. Our system enabled us to access the plume close to an active vent as well as the aged plume several kilometers downwind of the source and elevated from ground, without exposing operators to the risks in proximity to active vents or employing manned aircrafts to potential engine-damaging ash and gas plumes. In addition to that, the UAV deployment of a lightweight DOAS instrument for SO_2 flux estimations is presented herein, which enables fast plume traversing in terrain that is usually not accessible by car or even by foot.

2 Site description

2.1 Stromboli

Stromboli volcano, the northernmost island of the Aeolian volcanic arc (Italy), rises 924 m above sea level (a.s.l.). The island represents the top part of a large 2500 m high stratovolcano emerging from the Tyrrhenian Sea floor. Stromboli is well known for its regular ($\sim$ every 10–20 min) explosive activity (Strombolian activity). Intermittently, continuous passive degassing occurs from the active vents, which are located in the crater terrace at about 750 m a.s.l. Ejected lava material is dominantly deposited in a northwestern direction, forming a horseshoe-shaped area (Sciara del Fuoco) that is not safely accessible on foot. The summit above the craters is easily accessible, and numerous monitoring stations have been installed here for continuous observation of the ongoing

volcanic activity. Thus, Stromboli has been a laboratory volcano for studying magma degassing processes (Allard et al., 2008) and field testing new instrumentations for many years.

While most gas-monitoring station positions benefit from a northwesterly wind direction, a southeasterly wind only allows gas plume detection by spectroscopic methods. In this study, due to the dominance of southeasterly winds in early April 2016 an approach from an easterly direction was chosen, using a multicopter as a carrier for gas sampling and sensing instruments. The UAV was mostly launched at the northern shelter (see Fig. 1).

2.2 Masaya

Masaya volcano (elevation $\sim$ 600 m a.s.l.), Nicaragua, is a basaltic andesite shield volcano caldera (6×11 km in size) with a set of vents. The currently active vent is situated in the Santiago pit crater, formed in 1858–1859 (McBirney, 1956). Masaya persistently emits voluminous quantities of SO_2, with fluxes typically ranging from 500 to 2500 T d^{-1} (Mather et al., 2006; de Moor et al., 2013; Carn et al., 2017), currently making this volcano one of the largest contributors of volcanic gas emissions in the Central American Volcanic Arc (de Moor et al., 2017). The reappearance of a superficial lava lake ($\sim 40 \times 40$ m) at Masaya in January 2016 marked an increase in degassing activity. Due to high emission rates and the low-altitude plume, Masaya volcano has a detrimental environmental impact on the downwind areas, diminishing vegetation and potentially affecting human health (Delmelle et al., 2002). Continuous monitoring of the gas emissions is realized by a stationary MG system (through the Deep Carbon Observatory – Deep Earth Carbon Degassing initiative, DCO-DECADE) at the crater rim and two scanning DOAS instruments (Network for Observation of Volcanic and Atmospheric Change (NOVAC); Galle et al., 2010) in the downwind direction. Besides the presence of a strong plume, Masaya volcano provides perfect conditions for field testing new methods and studying plume chemistry using UAVs: it is easily accessible by car, at a low altitude, and has a relatively stable dominant wind direction (northeast). In July 2016 flights were launched from the caldera bottom, marked "flight area" in Fig. 2c.

2.3 Turrialba

Turrialba is a stratovolcano with a peak elevation of 3340 m a.s.l. and is located about 35 km east and directly upwind of San José, the capital of Costa Rica. It is the southernmost active volcano of the Central American Volcanic Arc. In the 2000s, an almost 150-year-long period of quiescence ended and since 2010 several vent opening phreatic eruptions have occurred, marking an ongoing but erratic phase of unrest (Martini et al., 2010) characterized by variable ash and gas emission intensities (up to 5000 tons day^{-1} of SO_2; de Moor et al., 2016a). This made Turrialba volcano the second

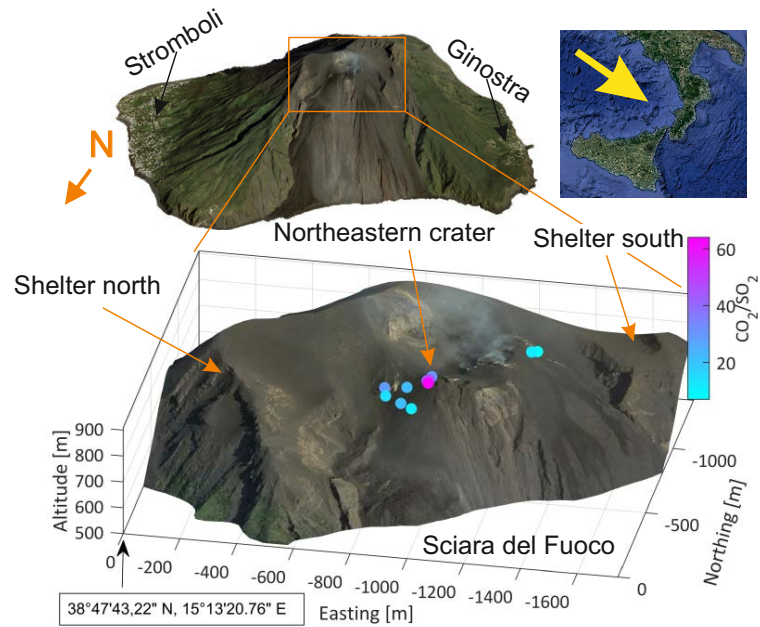**Figure 1.** Overview of the sampling site at Stromboli volcano with the locations of the retrieved CO_2 / SO_2 mixing ratios given in Table 2.
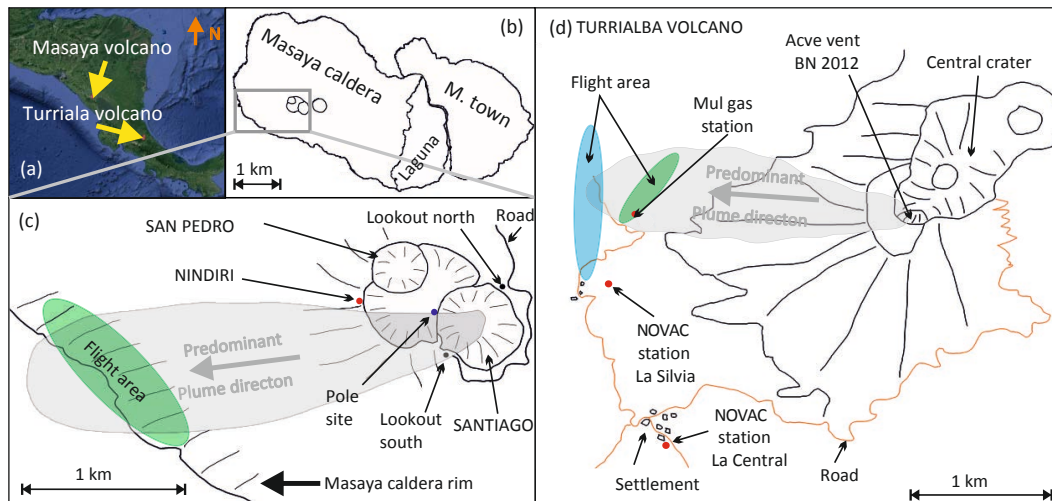

Figure 2. Overview of the fieldwork sites at **(a–c)** Masaya volcano (Nicaragua) and **(d)** Turrialba volcano (Costa Rica). Sampling locations mentioned in Table 3 are marked in **(c)** as follows: Santiago rim, lookout south (black marker); Santiago rim, pole site (blue marker); Nindiri rim (red marker).

most substantial emitter in the arc, besides Masaya volcano (de Moor et al. 2017). The proximity of Turrialba volcano to the densely populated central valley, which has Costa Rica's major international airport, and the dominant western wind direction is responsible for ash depositions, causing health and air traffic problems. Therefore, the activity of Turrialba is continuously monitored by various systems including permanent Multi-GAS stations to observe short-term precursory changes in the gas composition prior to eruptive events (de Moor et al., 2016a). However, stations located near the ac-

tive vent suffer from ash deposition and ballistic impacts during more frequent episodes, making maintenance demanding and risky or impossible. Furthermore, the accessibility of the summit and surrounding areas is decreasing due to intense erosion following vegetation destruction by acid rain, heavy rainfall, ash deposition and remobilization, and the lack of infrastructural maintenance following community evacuation. Thus, the use of UAV-based systems might represent the only viable approach for in situ measurements of the open-vent plume during periods of high activity. In 2016 flights
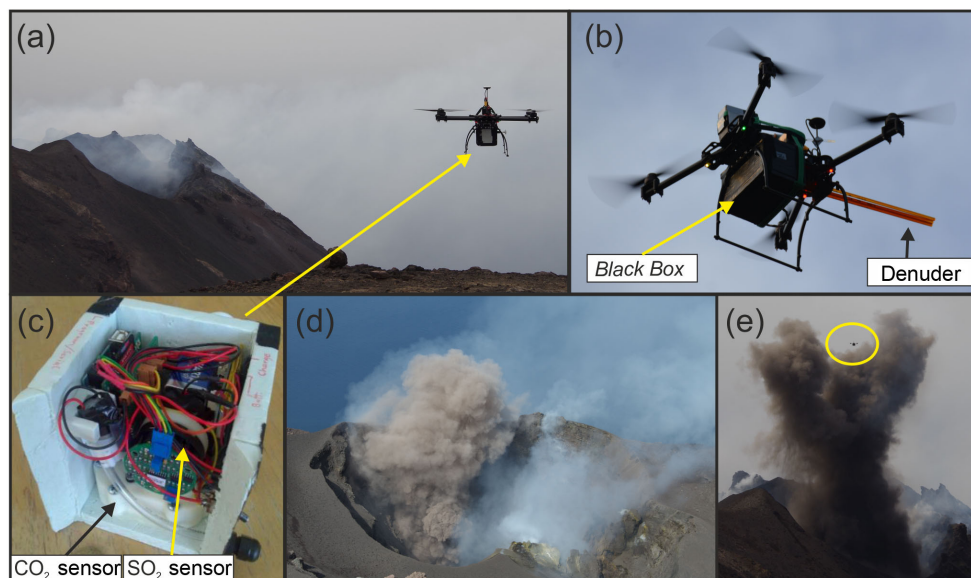
Figure 3. (a) Sampling site at Stromboli volcano with the northeastern crater in the background and the RAVEN UAV carrying the Sunkist gas monitor, **(b)** RAVEN UAV with the black box sampling unit and three gas diffusion denuders, **(c)** interior view of the Sunkist gas monitor, showing the CO_2 and SO_2 sensors, **(d)** passive degassing (white plume) and eruptive ash explosion (brown ash cloud) at the northeastern crater at Stromboli volcano, **(e)** ash eruption at the northeastern crater producing an ascending ash plume with the RAVEN UAV in direct proximity (yellow circle), returning from sampling flight.

were conducted starting at the La Silvia site (Fig. 2d) to investigate the feasibility of a UAV-based gas sensing system in this challenging environment (high altitude and thick ash plumes).

3 Instrumentation

3.1 Unmanned aerial vehicle

The UAV (called RAVEN, remote-controlled aircraft for volcanic emission analysis; see Fig. 3a–b) used during the field campaigns was a four-rotor multicopter with foldable arms (Black Snapper, Globe Flight, Germany) and an E800 motor set using propellers with a diameter of 13 inch (0.33 m) and a pitch of 4.5 inch (0.11 m) (DJI Innovations, Shenzhen, China). It was flown manually in line-of-sight conditions. The multicopter had a weight of 2.3 kg including a 22.2 V (6S) 4.5 Ah battery. A maximum payload of 1.3 kg was achieved with various mounted instruments. The foldable frame of the UAV was beneficial with regards to the usual requirement of personally carrying equipment into the field, especially on volcanoes like Stromboli. Another advantage of this system was that the battery capacity is within the guidelines of air travel restrictions, allowing the system to be transported on commercial airplanes. The main controller (NAZA M-2, DJI Innovations, Shenzhen, China) of the multicopter was connected to a combined denuder sampling and SO_2 sensing instrument (hereafter named black box; see Sect. 3.3) to transmit the measured SO_2 data as an 0–5 V signal to the remote control, where it is displayed. This allowed the operator to find areas with dense plumes in which to hover the system for stationary sampling and to react to changes in the plume direction. This is challenging if relying only on visual observation of the plume. A data logger (Core 2, Flytrex Aviation, Tel Aviv, Israel) with a micro SD card was used to log the flight data from the main controller consisting of GPS coordinates, pressure and temperature data at 2 Hz. The payloads were attached below the main body of the multicopter with an inlet for the in situ CO_2 and SO_2 sensing instrument (hereafter called Sunkist; see Sect. 3.2), close to the center of the copter. The sampled air volume can be assumed to originate from within a radius of a few meters around the inlet (see e.g., Roldan et al., 2015; Alvarado et al., 2017; Palomaki et al., 2017), which represents homogeneous plume gas for a widely spread out plume. This assumption is confirmed by a self-developed method for the estimation of the origin of sample air, which is described in the Supplement (Sect. 4).

3.2 CO_2 / SO_2 gas sensors – Multi-GAS (Sunkist)

A gas sensor system was developed for use in volcanic environments with a focus on robustness and has a compact and lightweight design for application on UAVs. The system, called Sunkist (SK), contains two gas sensors:

1. A CO_2 sensor (K30 FR, SenseAir, Delsbo, Sweden) uses the principle of nondispersive infrared absorption
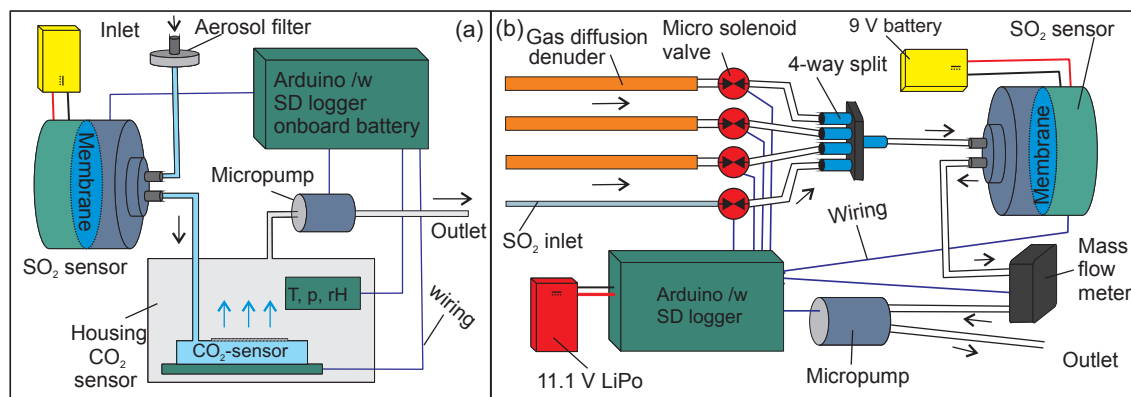
Figure 4. Schematics of the **(a)** Sunkist monitoring unit and the **(b)** black box gas sampling system.

spectroscopy: the sample gas gets sucked into a multi-reflection cell, where it is exposed to the radiation of a small infrared light source. The CO_2 concentration is determined by measuring the light attenuation on distinct CO_2 absorption bands in the near infrared.

2. An electrochemical SO_2 sensor (CiTiceL 3MST/F, City Technology, Portsmouth, United Kingdom) basically consists of an electrochemical cell, where oxidation of SO_2 on one of the cell's electrodes creates charges and leads to a measurable compensating current between the two cell electrodes.

The CO_2 sensor is placed inside a hermetic box, which is part of the air path (Fig. 4a). It is equipped with further on-chip sensors for humidity (SHT21 from Sensirion, Staefa, Switzerland), temperature and pressure (BMP180 by Bosch Sensortec, Reutlingen, Germany), which allow the gas data to be corrected for dependencies on named environmental parameters.

The sensors are read out by a custom-built Arduino Uno Rev 3 computer with a micro SD card logger at a sampling rate of 2 Hz and powered by a rechargeable 3.7 V lithium polymer (LiPo) battery (Fig. 4b). The SO_2 sensor was powered by a separate 9 V alkaline battery. The whole system is sheltered in a polystyrene foam case and has a total weight of 500 g (Fig. 3c). A 45 µm pore size PTFE filter was attached to the inlet to prevent particles from entering the sensors. Gas was pumped through to the sensors in series (1. SO_2, 2. CO_2) by a small pump using a flow rate of 500 mL min^{-1}. The system was calibrated before and after field deployments with CO_2 (0–1500 ppm) and SO_2 (0–30 ppm) test gases. Detailed information on the specifications of the sensors is shown in Table 1 and in the Supplement (Fig. S1).

3.3 Gas diffusion denuder sampler (black box)

An in situ gas sampling system was constructed to enable gas diffusion denuder sampling in the plume at various distances from the vent using the UAV. To compensate for dilution, a

CiTiceL 3MST/F SO_2 sensor (City Technology, Portsmouth, United Kingdom) was implemented to obtain halogen/sulfur ratios combining denuder samples and sensor data. The sampler (called black box – BB) consisted of the following components, which are introduced in the order the gas passes through:

1. inlet system for three denuders,

2. electrochemical SO_2 sensor,

3. mass flow sensor,

4. micro gas pump (see Fig. 4b and Table 1).

The housing was made of polystyrene foam to ensure that the weight requirements were met. An Arduino microcontroller (Uno Rev 3) for signal processing and data logging on a SD card was built in. Various 11.1 V LiPo batteries (500 and 1000 mAh) supplied the power, with different capacities depending on the desired payload and operation time. The Arduino computer transmitted a pulse width modulated signal between 0 and 5 V, proportional to the detected SO_2 mixing ratio, to the main controller of the multicopter via cable connection, which then was sent by telemetry to the remote control to allow the operator to assess plume strength in real time to optimize denuder exposure time. The SO_2 gas sensor was calibrated in the laboratory and close to field conditions with SO_2 gas standards in N_2 (0–54.1 ppm).

Gas diffusion denuder sampling, which enriches gaseous compounds while being insensitive to the particle phase, was applied by using two types of coating materials as derivatization agents for the gas diffusion sampling. Total gaseous reactive molecular bromine species, Br^x (Br_2, BrCl, (H)OBr), were determined by denuders coated with 15 µmol of 1,3,5-trimethoxybenzene (TMB) – which reacts to 1-bromo-2,4,6-trimethoxybenzene – and subsequent gas chromatography-mass spectrometry (GC-MS) analysis (Rüdiger et al., 2017). Hydrogen bromide (HBr) was sampled with denuders coated with 7.2 µmol of 5,6-epoxy-5,6-dihydro-1,10-phenanthroline

Table 1. Components and specifications of the sampling and sensing instruments.

Component/parameter	Specifications			
	Sunkist		Black box	
CO_2 sensor	NDIR, SenseAir CO_2 Engine K30 FR			
SO_2 sensor	Electrochemical, CiTiceL 3MST/F		Electrochemical, CiTiceL 3MST/F	
Operating temperature	0–50 °C (CO_2), −2–50 °C (SO_2)		−20–50 °C	
Operating humidity	0–95 % (CO_2), 15–90 % (SO_2), noncondensing		15–90 % (SO_2), noncondensing	
Operating pressure	Atmospheric ± 10% (SO_2)		Atmospheric ± 10%	
Temperature dependence	$1/T$ (assumed for CO_2), 0.25 % °C^{-1} (SO_2)		0.25 %/° C	
Pressure dependence	1.6 %/kPa (CO_2), 0.0015 %/kPa (SO_2)*		0.0015 % kPa^{-1}*	
Response time	2 s (CO_2), < 20 s (SO_2)		< 20 s	
Accuracy	±30 ppm ± 5 % signal (CO_2), ±1 ppm ± 1 % signal (SO_2)		±1 ppm ± 1 % signal	
Instrument noise (1σ)	5 ppm (CO_2), 0.05 ppm (SO_2)		0.05 ppm	
Range	0–5000 ppm (CO_2), 0–200 ppm (SO_2)		0–100 ppm	
Sampling rate	2 Hz		2 Hz	
Computer	Arduino, with micro SD card logger		Arduino, with SD card data logger and p motor-shield to power the pum	
Voltage	9 V for SO_2 sensor (alkaline battery), 3.7 V LiPo battery for Arduino		9 V for SO_2 sensor (alkaline battery), 11.1 V LiPo battery for Arduino and pump	
Inlet	Particle filter		3 denuders (50 cm) or 3 × 2 denuders (15 cm)	
Others	Warm up time	1 min (CO_2)	Micro solenoid valves	First Sensor, Germany TN2P006LM05LB
	Additional sensors	Temperature, pressure, relative humidity	Mass flow meter	First Sensor, Germany, WBAL001DUH0
			Micro pump	TCS micropumps, UK, DS250BL
Weight	500 g		500 g	
dimensions	14 × 13 × 14 cm (L × W × H)		20 × 13 × 14 cm (L × W × H)	

* The pressure dependence of 0.0015 % kPa^{-1} is a second-order effect and is negligible for our application.

(EP) – which is selectively reactive towards halogen acids through its epoxy function, forming 5-halogeno-6-hyrdroxy-5,6-dihydro-1,10-phenanthroline – and analyzed by liquid chromatography mass spectrometry (LC-MS). For the UAV-based application 15 cm long denuders were used at a sampling flow rate of 208 mL min^{-1} to ensure quantitative sampling. Denuders with both coating types were sampled at the same flow rate simultaneously with the recording of Multi-GAS (Sunkist) data.

3.4 Drone-operated miniature differential optical absorption spectroscopy (DROAS)

A miniature UV spectrometer system (Galle et al., 2003) was employed to fly mobile DOAS traverse measurements which could conduct estimations of the SO_2 flux at Turrialba volcano. This system consisted of an UV spectrometer (Fig. 8a; USB2000+, Ocean Optics, USA), a miniature

telescope (Ocean Optics 74-DA collimating lens, diameter: 5 mm, focal length 10 mm), a GPS antenna (BU-353-S4, GlobalSat, Taipei, Taiwan) and a miniature on-board computer (VivoStick TS10, ASUS, Taipei, Taiwan). The system was powered by a 11.1 V LiPo battery (1000 mAh), which was connected via a switching regulator (CC BEC 10 A, Castle Creations, USA) to give 9 V at 2 A. The spectrometer and the GPS antenna were connected (and powered) at the computer via USB ports. The NOVAC mobile DOAS software developed at the Chalmers University (Sweden) was run on the computer for data acquisition and later for evaluation. The miniature PC in the spectrometer system was accessed via a remote desktop connection on a different computer to initialize the data acquisition by the mobile DOAS" software. Validation of the SO_2 fluxes obtained by DROAS traverses was achieved by comparison with the SO_2 fluxes derived by

two NOVAC stationary DOAS instruments (La Silvia and La Central; see Fig. 2d) located in proximity to the flight area.

3.5　Data processing

3.5.1　Sensor calibration

All three in situ gas sensors (two identical SO_2, one CO_2) were calibrated using test gas standards mixed with nitrogen, using either tedlar bags, dynamic dilution or readily mixed test gases. The sensors were exposed to different mixing ratios by pumping the gas mixtures through the system. Calibration functions were fitted, including errors in mixing ratio and signal (York et al., 2004) to give sensitivities (slope) and offset levels (intercept) (Supplement Figs. S2–S4). As the CO_2 sensor responds to the gas concentration (molecules per volume), CO_2 mixing ratios (molecules per molecules of air) were obtained by compensating for the concentration signals with pressure and temperature data recorded by the built-in sensors, assuming ideal gas behavior. The SO_2 sensor output, however, relates directly to the mixing ratio due to the diffusivity of the transport membrane being inversely proportional to the pressure and therefore canceling out the pressure dependency of the concentration. The two gas sensors operate with significantly different response times (T_{90} for $CO_2 \sim 2\,s$, for $SO_2 \sim <20\,s$), since the sample gas enters the SO_2 sensor only by molecular diffusion, whereas in the CO_2 sensor it is directly driven through the optical cell. In order to adjust the response times of the two sensors, a slow response signal for the CO_2 sensor ($CO_{2,sim}$) was simulated. This was achieved through convolution of the original signal with a typical sensor pulse response,

$$f(t) = \begin{cases} 0, & t < 0 \\ \dfrac{1}{\tau} e^{-t/\tau}, & t \geq 0 \end{cases},$$

with t being time and τ being the response-time factor, which in this context can be regarded as a measure for the degree of smoothing. The approach is mathematically equivalent to an approach shown by Roberts et al. (2014). The response-time factor τ was tuned, such that the correlation of $CO_{2,sim}$ and SO_2 signal were maximized for discrete peaks (see Fig. 5a). This was already done by Arellano et al. (2017), who also applied the Sunkist instrument to gas measurements in Papua New Guinea in 2016.

3.5.2　Gas diffusion denuder analysis

The sampled gas diffusion denuders were sealed in air-tight containers and stored in darkness for subsequent analysis. The coating, which contained the derivate and derivatization agent in excess (TMB or EP), was eluted off the denuders using 5 times 2 mL of 1:1 of ethyl acetate and ethanol (in the case of TMB) or 5 times 2 mL methanol (EP). After the elution, the solvent was evaporated (at 35 °C under gentle N_2 gas stream) to a volume of approximately 100 µL.

Internal standards (with TMB: 2,4,6-tribromoaniline; with EP: neocuproine) were added to each sample solution to account for evaporation losses. The condensed samples were analyzed by GC-MS (TMB) and LC-MS (EP) and quantified using external calibration. Due to the lack of a pure calibration, standard hydrogen bromide was only measured qualitatively. Halogen mixing ratios in air were derived from the measured halogen amounts on the denuders and the respective sampling volume obtained by the sampling pump data. In addition to the actual sample denuders, open-field blank denuders were prepared to account for potential diffusive gas precipitation during the flights.

3.5.3　Gas ratios

For a feasible data interpretation, gas ratios were calculated from the sensor data and the denuder analysis results. Halogen mixing ratios were interpreted concerning dilution with ambient air by relating to SO_2, which is rather slow in its oxidation, and therefore can be treated as a stable dilution proxy for a short-term plume observation (Porter et al., 2002). Thus, the derived halogen mixing ratio was divided by the time-integrated SO_2 mixing ratios obtained during the denuder sampling period to obtain Br_x / SO_2 ratios. Due to a baseline drift in the CO_2 sensor data, which were only observable during long-term measurements ($> 45\,min$), the pressure- and response-time-corrected CO_2 data were additionally drift corrected for long-term measurements. A linear fit was made to the sloped background signal and subtracted from the CO_2 signal (see Supplement Fig. S5). CO_2 / SO_2 ratios were calculated with a linear fit to CO_2 vs. SO_2 scatter plots, considering the deviations (York et al., 2004) of the two sensor signals.

3.5.4　DROAS evaluation and gas fluxes

SO_2 emission rates during the flights at Turrialba were derived by traversing the plume with the DROAS instrument pointing vertically upwards in the direction of the plume. The mobile DOAS software developed at Chalmers University was used to control the spectrometer and to retrieve SO_2 column amounts from the spectra. The SO_2 columns were achieved using a wavelength evaluation window of 310–330 nm and included O_3 and SO_2 absorption cross sections convoluted with a slit function as well as a ring spectrum and a third-order polynomial in the DOAS fitting routine. The calculation of the SO_2 emission rate involves the integration of the SO_2 column amounts measured along the flight path, resulting in a cross-sectional SO_2 area, which was geometrically corrected to obtain a surface that is orthogonal to the plume direction, and then multiplied by the wind speed (obtained from the NOAA National Center for Environmental Predictions (NCEP) Global Forecast System) to calculate SO_2 fluxes. Further details on the spectral evaluation routines
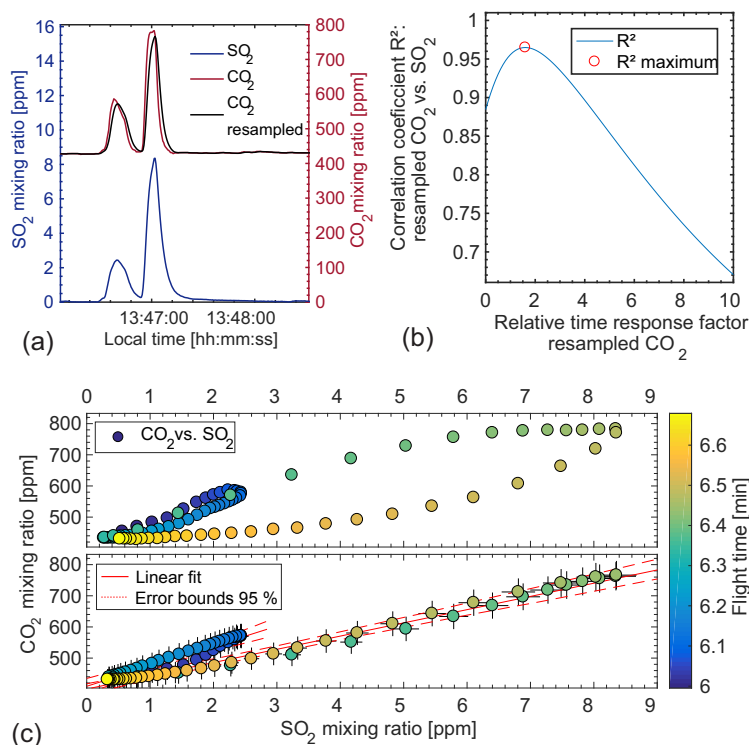
Figure 5. (a) Example of time series for mixing ratios of SO_2 and CO_2 (original data in red, resampled data in black), showing discrete gas masses at Stromboli volcano (first flight on 5 April 2016), (b) Correlation plot for the determination of the relative response-time factor for the CO_2 gas sensor with a maximum at a relative response-time factor of 1.7, (c) CO_2 over SO_2 mixing ratios, showing the outcome of the resampling of the fast CO_2 with a relative response-time factor of 1.7 (lower plot), linear regression results CO_2 / SO_2 ratios of 64 ± 16 the first peak and 42 ± 4 for the second.

and flux calculations can be found elsewhere (de Moor et al., 2017).

4   Results and discussion

4.1   Multicopter performance assessment

During the deployment at three volcanoes, the RAVEN multicopter conducted more than 50 flights under moderate wind conditions, in most cases below $10 \, \text{m s}^{-1}$. The multicopter achieved a maximum operation altitude of 3320 m at Turrialba volcano and records showed a maximum speed of $85 \, \text{km h}^{-1}$. With a takeoff weight of 2.45 kg and a payload of maximum 1.3 kg flights at Turrialba volcano were still possible, although the flight time was reduced to about 5 to 8 min. At the Masaya volcano sites (takeoff altitude ~ 500 m), a maximum ascent above ground level of 1080 m was recorded. A typical flight time at this site was between 10 and 15 min. The telemetrically transmitted SO_2 mixing ratios from the black box apparatus allowed the localization of high plume densities and therefore adjustments on the optimal hover location. While flying in the line of sight the system could be reliably controlled within a distance of 1–2 km

to the operator. However, entering the dense plume proved to challenge the connection between the remote control and the receiver, resulting in multiple connection losses during flights, in which the UAV also left the line of sight of the operator. Nevertheless, a GPS connection was still present and an automated return mechanism allowed control to be regained after the UAV left areas of high plume densities. At Masaya this phenomenon was observed mostly in a plume with condensed water and SO_2 mixing ratios in low one-digit ppmv numbers, while in a plume without condensation close to the crater, control was maintained even with SO_2 levels up to 40 ppmv. This is probably due to the attenuation effect of fog and cloud droplets on millimeter waves, as they are used with the 2.4 Ghz transmitter of the remote control (Zhao and Wu, 2000).

4.2 CO_2 / SO_2 gas sensors

During two field deployments, at the Stromboli (Table 2) and Masaya (Table 3) volcanoes, the lightweight gas-monitoring system SK determined CO_2 / SO_2 gas ratios at various airborne and ground-based locations. A comparison with a stationary MG instrument at Masaya volcano for the same site and time (lookout point south, 14 July 2016, 11 : 19) and with

Table 2. Overview of the retrieved CO_2 / SO_2 ratios with parameters for the linear fit at Stromboli volcano.

Date	Time	Flight/ peak	CO_2 / SO_2	Lower SO_2 limit/ppmv	Data points	Max. SO_2/ ppmv	Estimated distance/m
05.04	13:46	1/1	64 ± 16	1	39	2.6	26
05.04	13:46	1/2	42 ± 4	1	48	8.5	11
05.04	14:31	2/1	43 ± 8	1	31	4.5	18
05.04	14:32	2/2	31 ± 12	1	29	4.7	25
05.04	16:18	3/1	7 ± 5	0.1	101	5.8	419
05.04	16:23	3/2	11 ± 11	0.1	133	1.9	399
06.04	13:03	4/1	27 ± 25	0.2	326	0.9	155
06.04	13:44	5/1	22 ± 5	0.5	324	5.2	80
06.04	14:44	6/1	10 ± 13	0.2	111	1.6	170
06.04	14:45	6/2	21 ± 7	0.5	415	2.3	177
06.04	15:10	7/1	9 ± 5	0.2	516	1.6	167
06.04	15:16	7/2	21 ± 5	0.5	35	2.3	107

Table 3. CO_2 / SO_2 mixing ratios and calculation parameters obtained from the Sunkist (SK) and Multi-GAS (MG) instruments at Masaya volcano. The exact locations are given in Fig. 2; errors indicate 2σ interval (95.5 %) retrieved by a linear regression (York et al., 2004) including the measurement errors of both the SO_2 (error: 5–10 %) and CO_2 (error: 5.5 %) sensor.

Date	Time	Instrument	Location/flight	CO_2 / SO_2	Lower SO_2 limit/ppmv	Data points	Max. SO_2	Distance to rim/km
14.07.2016	09:43–15:10	MG	Santiago rim; lookout south	2.9 ± 0.1	4	3200	31.1	0
14.07.2016	11:18–11:44	MG	Santiago rim; lookout south	2.9 ± 0.3	4	440	17.5	0
14.07.2016	11:19–11:45	SK	Santiago rim; lookout south	3.8 ± 0.5	4	1460	17.9	0
14.07.2016	10:42– 12:09	SK	Santiago rim; lookout south	3.6 ± 0.4	4	2600	18.5	0
15.07.2016	09:43–16:23	MG	Santiago rim; pole site	3.1 ± 0.1	4	2950	29.6	0
15.07.2016	15:28–16:19	SK	Nindiri rim	3.3 ± 1.2	1	3100	5.8	0.5
16.07.2016	11:18–12:19	SK	Santiago rim; pole site	4.7 ± 0.3	4	3000	28	0
17.07.2016	08:56–08:59	SK	caldera valley; flight no. A2	2.9 ± 13	1	150	2.8	1.8
17.07.2016	11:21–11:28	SK	caldera valley; flight no. A5	4.8 ± 3.2	1	630	4.8	1.8
17.07.2016	11:53–12:01	SK	caldera valley; flight no. A6	6.5 ± 3.4	0.2	620	3.4	1.9
17.07.2016	12:10–12:20	SK	caldera valley; flight no. A7	6.2 ± 5.6	0.4	1150	2.2	1.5
18.07.2016	07:55–09:36	SK	Santiago rim; pole site	4.1 ± 0.3	4	4350	36.7	0
18.07.2016	13:19–13:27	SK	caldera valley; flight no. B4	5.1 ± 4	1	560	4.4	1.7
20.07.2016	12:55–13:04	SK	caldera valley; flight no. C1	7.5 ± 5.8	0.5	310	2.8	1.9
20.07.2016	13:29–13:35	SK	caldera valley; flight no. C2	7.7 ± 5.1	0.75	470	2.9	1.9
20.07.2016	13:58–14:07	SK	caldera valley; flight no. C3	2.2 ± 11	0.5	380	1.9	1.9
20.07.2016	16:22–16:29	SK	caldera valley; flight no. C7	5.3 ± 4.4	0.5	550	3.4	2

inlets of both systems in proximity to each other gave results on CO_2 / SO_2 ratios that were within each other's 2σ intervals (CO_2 / SO_2 of 2.9 ± 0.3 for MG and 3.6 ± 0.4 for SK). The time series of the SO_2 mixing ratios of SK and MG also showed good agreement ($R^2 = 0.89$) (Fig. 6). An application of SK further downwind (0.5 km from the rim) gave a CO_2 / SO_2 ratio of 3.3 ± 1.2, while the MG measured a CO_2 / SO_2 ratio of 3.1 ± 0.1 during the same time at the rim. This shows SK's ability to be deployed in a more diluted plume, but with the disadvantage of higher errors, due to the higher relative background in CO_2 at more distant locations. Furthermore, UAV-based application (nine flights, 17–20 July 2017) between 1.5 km and 2 km downwind of the Masaya plume resulted in 42 % higher CO_2 / SO_2 ratios on average with a larger standard deviation compared to the crater rim (14–16 July 2017), but still within each other's errors (CO_2 / SO_2: 5.4 ± 2.3 at 1.5–2 km; 3.8 ± 0.3 at the rim). Due to the limitations of the CO_2 sensing, acquiring useful CO_2 / SO_2 data with SK is more feasible in dense plumes close to the crater rim but not limited to it, as the airborne application has shown. Additionally, SO_2 mixing ratios were measured as a plume dilution proxy by the black box (BB) system. Both the BB and SK systems use an identical SO_2 sensor and showed a good agreement of their SO_2 time series and time-integrated SO_2 mixing ratio (SK: 1.75 ± 0.08 ppmv, BB: $1{,}84 \pm 0.08$ ppmv) (Supplement S6).

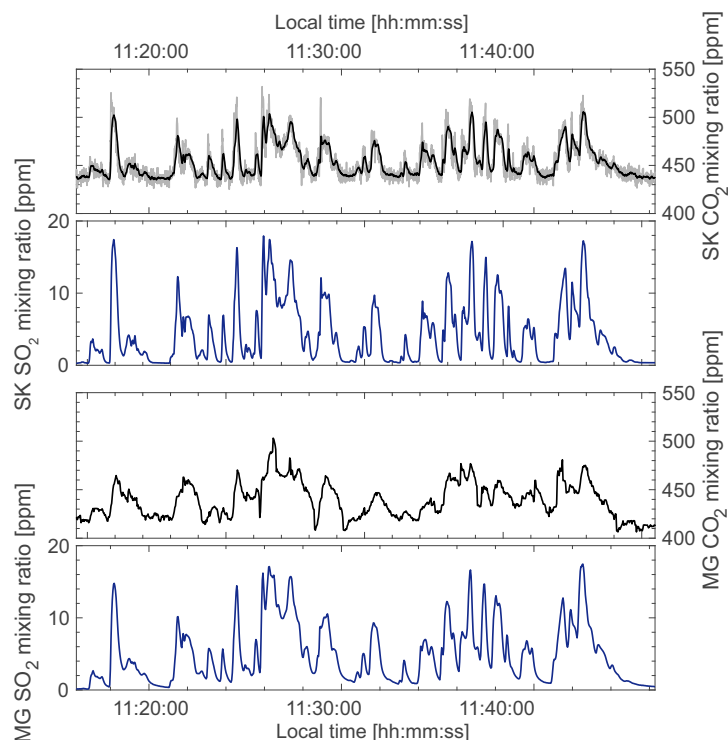At Stromboli volcano, the Sunkist and black box systems were deployed on 2 days (5 and 6 April 2016), resulting in

Figure 6. Comparison of SO_2 and CO_2 time series of a Multi-GAS (MG) instrument and the Sunkist (SK) unit at the Masaya volcano crater rim (for SK CO_2 raw data in grey, resampled data in black), both instrument inlets were placed in proximity to each other (14 July 2016); SK $CO_2 / SO_2 = 3.63 \pm 0.43$ (background $CO_2 = 439$ ppm); MG $CO_2 / SO_2 = 2.94 \pm 0.30$ (background $CO_2 = 413$ ppm); additional scatter plots in the Supplement.

seven flights into the plume. These flights covered distances of between 11 and 419 m from the vent in a downwind direction (northeast), above the Sciara del Fuoco. As shown in Fig. 1, discrete gas clouds with different CO_2 / SO_2 compositions were measured. The retrieved CO_2 / SO_2 ratios ranged between 7 and 64, with the higher values typically detected directly above the vent (11 to 26 m) (see Table 3 and Fig. 1). During the multicopter operations close to the vent regular strombolian ash explosions occurred (see Fig. 3d and e), which are likely accompanied by CO_2-rich gas clouds (La Spina et al., 2013) and therefore act as a possible explanation for the detected high CO_2 / SO_2 ratios. On both flight days the predominant wind direction was southwest ($207° \pm 15°$ and $210° \pm 18°$, data from weather station at 77 m a.s.l., commercially available from http://www.windfinder.com, Kiel, Germany), which resulted in the plume mostly being present across the Sciara del Fuoco and therefore only accessible by UAV. Nevertheless, a local Multi-GAS station (placed on the SE rim of the crater terrace) discontinuously measured the plume during the period of the UAV survey, showing CO_2 / SO_2 ratios between 2.2 and 13.6, which is in agreement with some of the multicopter-based measurements. Similar CO_2 / SO_2 ratios have been observed in the past and are exemplary for ordinary Strombolian activity (Aiuppa et

al., 2009). It has to be taken into account that both instruments did not measure simultaneously or in proximity to each other. The MG instrument only measures four times a day for 30 min and averages over this time, while with the SK instrument we identified discrete peaks of gas clouds with different CO_2 / SO_2 ratios. Furthermore, a comparison of SK and MG CO_2 / SO_2 data might be more accurate with the high SK CO_2 / SO_2 values (associated with eruptive degassing) left aside, as we lack the observations on passive or eruptive degassing behavior for the MG data records.

4.3 Halogen measurements

Bromine species were detected by gas diffusion denuder sampling on three of the seven flights at Stromboli volcano. Reactive bromine species were measured between 0.14 and 0.65 ppb (see Table 4), while HBr was determined qualitatively in all three samples.

The obtained ratios of reactive bromine (Br_x) to SO_2 (1.9×10^{-4}–9.8×10^{-4}) are within the range of bromine to sulfur ratios produced by other methods at Stromboli volcano, e.g., alkaline trap sampling by Wittmer et al. (2014) (4.3×10^{-4}–2.36×10^{-2}). Figure 7b shows the Br_x / SO_2 ratios for different plume ages, which was calculated by taking wind speeds into account. Although the general feasi-
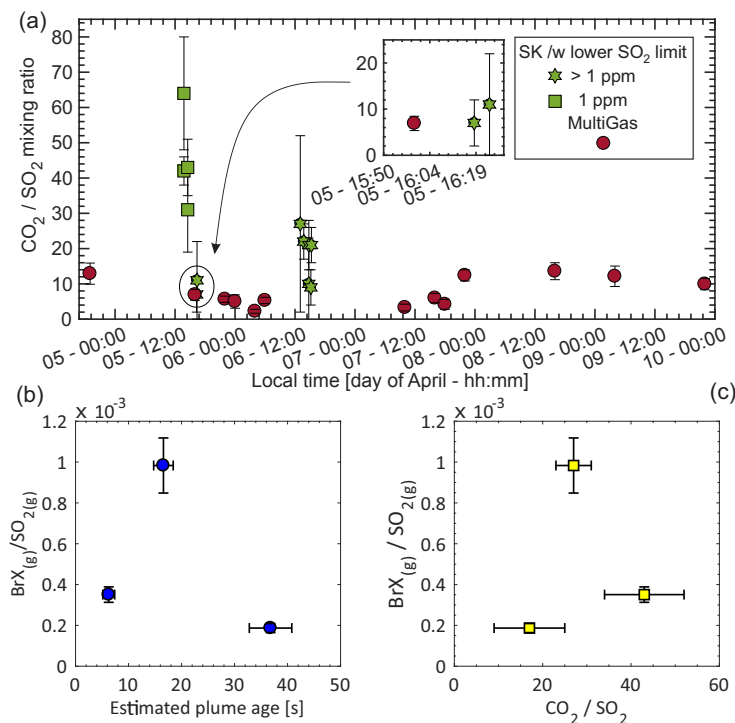
Figure 7. (a) Measured CO_2 / SO_2 gas ratios over a 5-day period by a Multi-GAS station (located east of the crater terrace) and airborne measurements with the Sunkist system at Stromboli volcano. Data point shapes indicate the lower SO_2 mixing ratio limits for the linear fit over the CO_2 vs. SO_2 data. **(b)** Development of the gaseous reactive bromine species over SO_2 over the estimated plume age (derived from distance to crater and estimated wind speed). **(c)** Gaseous reactive bromine / SO_2 ratios vs. CO_2 / SO_2 ratio.

Table 4. Sample parameter and bromine measurement results for three denuder samples at Stromboli volcano.

Sample number	1	2	3
Date	05.04.2016	06.04.2016	06.04.2016
Time	14:31	13:46	14:45
Duration /s	53	364	320
Sample volume/L	0.18	1.26	1.11
Pressure/mbar	906	914	914
Integrated SO_2/ppmv	1.85 ± 0.09	0.34 ± 0.04	0.74 ± 0.05
Br_x/ppb	0.65 ± 0.06	0.34 ± 0.01	0.14 ± 0.1
$Br_x / SO_2 \times 10^{-4}$	3.5 ± 0.4	9.8 ± 1.3	1.9 ± 0.2
CO_2 / SO_2	43 ± 9	27 ± 4	17 ± 8
Distance/m	21 ± 2	80 ± 2	177 ± 2
Wind speed/m s^{-1}	3.4 ± 0.5	4.8 ± 0.5	4.8 ± 0.5
Plume age/s	6 ± 1	17 ± 2	37 ± 4

bility of the used methods for the investigation of reactive halogen species in an aging plume is demonstrated in this proof-of-principle approach, a trend in the Br_x / SO_2 ratio over age is not recognizable for this limited data set. Without information on abundances of other halogen species such as $BrO_{(g)}$, $HBr_{(g)}$ and aqueous particulate bromine ($HBr_{(aq)}$), interpretation of the Br_x / SO_2 ratio is difficult, as the emitted gas composition may also change on shorter timescales

(La Spina et al., 2013) compared to the campaign duration. However, an increase in the reactive bromine species BrO with distance from the crater rim has previously been observed by DOAS measurements at various volcanoes and is well described in the literature (Oppenheimer et al., 2006; Bobrowski et al., 2007). Although the bromine speciation in volcanic plumes has been the subject of several ground-based (e.g., Gliß et al., 2015) airplane (e.g., General et al., 2015), satellite (e.g., Theys et al., 2009; Hörmann et al., 2013) and model studies (e.g., Bobrowski et al., 2007; Roberts et al., 2009, 2014; von Glasow, 2010; Jourdain et al., 2016) in recent years, in situ measurements are scarce. The data presented here for the first minute after emission highlight the potential for UAV-based measurements to improve the sample acquisition and thus obtain a better understanding of plume aging.

As shown in Fig. 7c, the Br_x to SO_2 ratio seems to change not only with the plume age but also with CO_2 / SO_2 mixing ratios, which were simultaneously obtained. However, with only three data points a further interpretation is inadequate due to the lack of a statistical basis. Nevertheless, these first results show the principal practicality of the used denuder sampling and gas sensing methods for simultaneous investigation of halogen, carbon and sulfur emissions.

Table 5. SO_2 fluxes obtained by DROAS traverses and two stationary scanning DOAS instruments at Turrialba volcano. The average fluxes from La Silvia and La Central were derived for a 2 h period in which the DROAS flights were conducted, maximum fluxes for this period as presented as well.

Instrument/traverse (unit)	SO_2 flux at $1\,\mathrm{m\,s^{-1}}$ ($\mathrm{T\,d^{-1}}$)	Error (%)	Wind speed ($\mathrm{m\,s^{-1}}$)	SO_2 flux ($\mathrm{T\,d^{-1}}$)
DROAS traverse A	419.9 ± 38.6	9.2	3.78 ± 2.62	1776 ± 1108
DROAS traverse B	381.6 ± 35.5	9.3	3.78 ± 2.62	1614 ± 1007
La Silvia NOVAC station AVERAGE	362.3 ± 72.5	20	3.78 ± 2.62	1533 ± 986
La Silvia NOVAC station MAX	481.72 ± 96.3	20	3.78 ± 2.62	2038 ± 1312
La Central NOVAC station AVERAGE	258.6 ± 51.7	20	3.78 ± 2.62	1094 ± 704
La Central NOVAC station MAX	448.1 ± 89.6	20	3.78 ± 2.62	1896 ± 1220

4.4 DROAS measurements

On 27 September, two DROAS plume transects were performed at Turrialba volcano during mild ash emission at around 2800 m a.s.l. with a total flight time of approximately 10 min. The flight was conducted in the downwind direction west of the active vent and crossed underneath the plume on a south–north axis (Fig. 8b), exiting the plume on both ends of the flight path, which is indicated by the low SO_2 column amounts close to the baseline in the northern- and southernmost section of the flight path (Fig. 8c). SO_2 fluxes were calculated for that flight and resulted in $1776 \pm 1108\,\mathrm{T\,d^{-1}}$ SO_2 for traverse A and $1616 \pm 1007\,\mathrm{T\,d^{-1}}$ SO_2 for traverse B (see Table 5). Calculation of the SO_2 fluxes obtained by the two scanning DOAS instruments from the NOVAC network, located on the southern edge of the plume, gave average results of 1533 ± 986 $\mathrm{T\,d^{-1}}$ SO_2 for La Silvia and $1094 \pm 704\,\mathrm{T\,d^{-1}}$ SO_2 from La Central for a 2 h period, in which the flight took place. Therefore, the results of the DROAS traverses are in good agreement with the scanning DOAS stations. De Moor et al. (2016a) conducted car-based mobile DOAS transects, which typically take ~ 45 min for a round trip due to rough terrain. Dynamic gas plumes can significantly change the plume's travel direction on scales of minutes, introducing a significant source of error to car traverses. A major advantage of the UAV method is that it is much quicker, about 10 min for a round trip, thus providing a more accurate snapshot of the plume.

5 Conclusion and outlook

In this study we have demonstrated the feasibility of a multicopter-based approach for volcanic in situ plume measurements to investigate the compositional variability of an aging plume. The use of a multicopter UAV proved to be a suitable alternative to ground-based operations, especially in hard to access or inaccessible areas, like active volcanic vents or elevated downwind plumes. The aerial sampling systems demonstrated robustness and effectiveness during the field missions with harsh environmental and meteorological
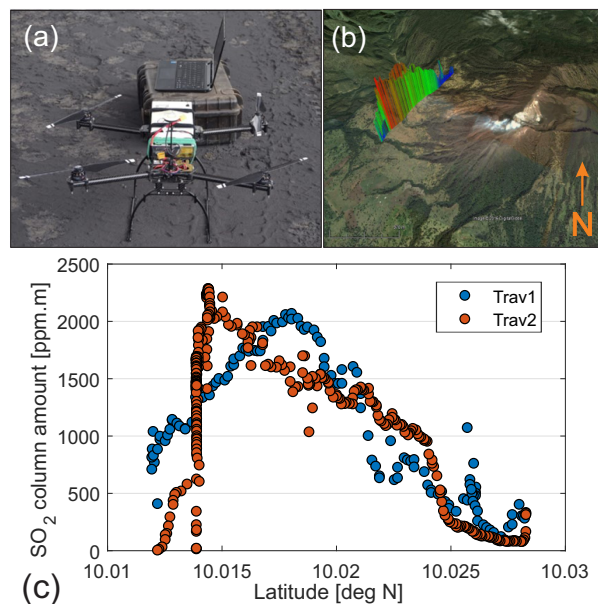

Figure 8. (a) Drone-operated miniature DOAS setup, **(b)** Illustration of SO_2 column amounts measured by DROAS at Turrialba volcano, **(c)** SO_2 column amounts during the transversal flight underneath the plume.

conditions, including ash-laden plumes. With the newly developed sampling system, reactive halogen species were observable in previously inaccessible downwind plume areas. Halogen speciation information enhances our understanding of plume chemistry in the aging plume, which represents important knowledge for new volcano-monitoring approaches. Therefore, in situ speciation methods for halogens should be extended and optimized for other gaseous and aqueous compounds including chlorine and iodine species. Additionally, at Stromboli volcano changes in the Br_x / SO_2 ratios were observed with different CO_2 / SO_2 ratios, which represent an interesting matter and should be further explored in future studies.

Furthermore, multicopter-based CO_2 / SO_2 ratio measurements showed their reliability, creating a promising approach

to monitoring inaccessible volcanoes or during dangerous eruptions minimizing personnel risk at highly active volcanoes. Although we demonstrated the applicability of the Sunkist lightweight gas sensing system for potential UAV-based monitoring, challenges in the acquisition of high-quality data for diluted plumes still exist. Thus, more sophisticated components (e.g., sensors, microcontroller or data logger) promise to achieve better sensitivities, but with the disadvantage of higher losses in the case of a crash.

Moreover, the UAV application presented here of a miniature DOAS instrument (DROAS) for SO_2 gas flux measurements has shown its quality in the harsh environment of Turrialba volcano. Its potential to be an excellent alternative to walking or car-based traverses for SO_2 flux acquisition has been proven with a significant reduction in risk and operation time.

The case studies presented here explored the general feasibility of multirotor UAVs in volcanic plume studies and are an initial step in the direction of remotely operated gas measurements at active volcanoes. We have shown the potential of UAV-based sampling to gain insights into reactive halogen chemistry and processes of plume aging, and further application of this method could yield data from previously physically inaccessible plume regions. Technological advances promise to enable scheduled, preprogrammed and autonomous UAV operations (e.g., from hangars close to volcanoes), with extended flight times for regular hazard assessments.

The Supplement related to this article is available online at https://doi.org/10.5194/amt-11-2441-2018-supplement.

References

Aiuppa, A., Federico, C., Giudice, G., Gurrieri, S., Liuzzo, M., Shinohara, H., Favara, R., and Valenza, M.: Rates of carbon dioxide plume degassing from Mount Etna volcano, J. Geophys. Res.-Sol. Ea., 111, B09207, https://doi.org/10.1029/2006JB004307, 2006.

Aiuppa, A., Moretti, R., Federico, C., Giudice, G., Gurrieri, S., Liuzzo, M., Papale, P., Shinohara, H., and Valenza, M.: Forecasting Etna eruptions by real-time observation of volcanic gas composition, Geol., 35, 1115–1118, https://doi.org/10.1130/G24149A.1, 2007.

Aiuppa, A., Federico, C., Giudice, G., Giuffrida, G., Guida, R., Gurrieri, S., Liuzzo, M., Moretti, R., and Papale, P.: The 2007 eruption of Stromboli volcano: Insights from real-time measurement of the volcanic gas plume CO_2/SO_2 ratio, J. Volcanol Geotherm. Res., 182, 221–230, https://doi.org/10.1016/j.jvolgeores.2008.09.013, 2009.

Aiuppa, A., Fischer, T. P., Plank, T., Robidoux, P., and Di Napoli, R.: Along-arc, inter-arc and arc-to-arc variations in volcanic gas CO_2/ST ratios reveal dual source of carbon in arc volcanism, Earth-Sci. Rev., 168, 24–47, https://doi.org/10.1016/j.earscirev.2017.03.005, 2017.

Allard, P., Carbonnelle, J., Dajlevic, D., Le Bronec, J., Morel, P., Robe, M. C., Maurenas, J. M., Faivre-Pierret, R., Martin, D., Sabroux, J. C., and Zettwoog, P.: Eruptive and diffuse emissions of CO_2 from Mount Etna, Nature, 351, 387–391, https://doi.org/10.1038/351387a0, 1991.

Allard, P., Aiuppa, A., Burton, M., Caltabiano, T., Federico, C., Salerno, G., and La Spina, A.: Crater gas emissions and the magma feeding system of Stromboli volcano, in: The Stromboli Volcano: An Integrated Study of the 2002–2003 Eruption, edited by: Calvari, S., Inguaggiato, S., Puglisi, G., Ripepe, M., and Rosi, M., American Geophysical Union, Washington, D.C., Geophysical Monograph Series, 182, 65–80, https://doi.org/10.1029/182GM07, 2008.

Altstädter, B., Platis, A., Wehner, B., Scholtz, A., Wildmann, N., Hermann, M., Käthner, R., Baars, H., Bange, J., and Lampert, A.: ALADINA – an unmanned research aircraft for observing vertical and horizontal distributions of ultrafine particles within the atmospheric boundary layer, Atmos. Meas. Tech., 8, 1627–1639, https://doi.org/10.5194/amt-8-1627-2015, 2015.

Alvarado, M., Gonzalez, F., Erskine, P., Cliff, D., and Heuff, D.: A Methodology to Monitor Airborne PM_{10} Dust Particles Using a Small Unmanned Aerial Vehicle, Sensors, 17, 343, https://doi.org/10.3390/s17020343, 2017.

Arellano, S., Galle B., Mulina K., Wallius, J., McCormick, B., Salem, L., D'aleo, R., Itikarai I., Tirpitz, L., Bobrowski, N., and Aiuppa, A.: Recent observations of carbon and sulfur gas emissions from Tavurvur, Bagana and Ulawun (Papua New Guinea) with a combination of ground and air-borne direct and remote sensing techniques, Abstract EGU2017-13644 presented at 2017 General Assembly, EGU, Vienna, Austria, 23–28 April 2017.

Bobrowski, N. and Giuffrida, G.: Bromine monoxide/sulphur dioxide ratios in relation to volcanological observations at Mt. Etna

2006–2009, Solid Earth, 3, 433–445, https://doi.org/10.5194/se-3-433-2012, 2012.

Bobrowski, N., Glasow, R. von, Aiuppa, A., Inguaggiato, S., Louban, I., Ibrahim, O. W., and Platt, U.: Reactive halogen chemistry in volcanic plumes, J. Geophys. Res., 112, D06311, https://doi.org/10.1029/2006JD007206, 2007.

Bobrowski, N., Giuffrida, G. B., Arellano, S., Yalire, M., Liotta, M., Brusca, L., Calabrese, S., Scaglione, S., Rüdiger, J., Castro, J. M., Galle, B., and Tedesco, D.: Plume composition and volatile flux of Nyamulagira volcano, Democratic Republic of Congo, during birth and evolution of the lava lake, 2014–2015, Bull. Volcanol., 79, B09207, https://doi.org/10.1007/s00445-017-1174-0, 2017.

Burton, M. R., Sawyer, G. M., and Granieri, D.: Deep Carbon Emissions from Volcanoes, Rev. Mineral. Geochem., 75, 323–354, https://doi.org/10.2138/rmg.2013.75.11, 2013.

Carn, S. A., Fioletov, V. E., McLinden, C. A., Li, C., and Krotkov, N. A.: A decade of global volcanic SO$_2$ emissions measured from space, Sci. Reports, 7, 44095, https://doi.org/10.1038/srep44095, 2017.

Carroll, M. R. and Holloway, J. R.: Volatiles in Magmas, in: Reviews in Mineralogy, vol. 30, Mineralogical Society of America, Washington, USA, 1994.

de Moor, J. M., Fischer, T. P., Sharp, Z. D., King, P. L., Wilke, M., Botcharnikov, R. E., Cottrell, E., Zelenski, M., Marty, B., Klimm, K., Rivard, C., Ayalew, D., Ramirez, C., and Kelley, K. A.: Sulfur degassing at Erta Ale (Ethiopia) and Masaya (Nicaragua) volcanoes: Implications for degassing processes and oxygen fugacities of basaltic systems, Geochem. Geophy. Geosy., 14, 4076–4108, https://doi.org/10.1002/ggge.20255, 2013.

de Moor, J. M., Aiuppa, A., Avard, G., Wehrmann, H., Dunbar, N., Muller, C., Tamburello, G., Giudice, G., Liuzzo, M., Moretti, R., Conde, V., and Galle, B.: Turmoil at Turrialba Volcano (Costa Rica): Degassing and eruptive processes inferred from high-frequency gas monitoring, Journal of geophysical research, Solid Earth, 121, 5761–5775, https://doi.org/10.1002/2016JB013150, 2016a.

de Moor, J. M., Aiuppa, A., Pacheco, J., Avard, G., Kern, C., Liuzzo, M., Martínez, M., Giudice, G., and Fischer, T. P.: Short-period volcanic gas precursors to phreatic eruptions: Insights from Poás Volcano, Costa Rica, Earth Planet. Sc. Lett., 442, 218–227, https://doi.org/10.1016/j.epsl.2016.02.056, 2016b.

de Moor, J. M., Kern, C., Avard, G., Muller, C., Aiuppa, A., Saballos A., Ibarra, M., LaFemina, P., Protti, M., and Fischer, T. P.: A new sulfur and carbon degassing inventory for the Southern Central American Volcanic Arc: The importance of accurate time-series datasets and possible tectonic processes responsible for temporal variations in arc-scale volatile emissions, Geochem. Geophy. Geosy., 18, 4437–4468, https://doi.org/10.1002/2017GC007141, 2017.

Delmelle, P., Stix, J., Baxter, P., Garcia-Alvarez, J., and Barquero, J.: Atmospheric dispersion, environmental effects and potential health hazard associated with the low-altitude gas plume of Masaya volcano, Nicaragua, Bull. Volcanol., 64, 423–434, https://doi.org/10.1007/s00445-002-0221-6, 2002.

Diaz, J. A., Pieri, D., Wright, K., Sorensen, P., Kline-Shoder, R., Arkin, C. R., Fladeland, M., Bland, G., Buongiorno, M. F., Ramirez, C., Corrales, E., Alan, A., Alegria, O., Diaz, D., and Linick, J.: Unmanned aerial mass spectrometer systems for in-situ volcanic plume analysis, J. Am. Soc. Mass Spectrom., 26, 292–304, https://doi.org/10.1007/s13361-014-1058-x, 2015.

Dinger, F., Bobrowski, N., Warnach, S., Bredemeyer, S., Hidalgo, S., Arellano, S., Galle, B., Platt, U., and Wagner, T.: Periodicity in the BrO / SO$_2$ molar ratios in the volcanic gas plume of Cotopaxi and its correlation with the Earth tides during the eruption in 2015, Solid Earth, 9, 247–266, https://doi.org/10.5194/se-9-247-2018, 2018.

Faivre-Pierret, R., Martin, D., and Sabroux, J. C.: Contribution des Sondes Aérologiques Motorisées à l'Etude de la Physico-Chimie des Panaches Volcaniques, Bull. Volcanol, 43, 473–485, https://doi.org/10.1007/BF02597686, 1980.

Galle, B., Johansson, M., Rivera, C., Zhang, Y., Kihlman, M., Kern, C., Lehmann, T., Platt, U., Arellano, S., and Hidalgo, S.: Network for Observation of Volcanic and Atmospheric Change (NOVAC) – A global network for volcanic gas monitoring: Network layout and instrument description, J. Geophys. Res., 115, 151, https://doi.org/10.1029/2009JD011823, 2010.

Galle, B., Oppenheimer, C., Geyer, A., McGonigle, A. J., Edmonds, M., and Horrocks, L.: A miniaturised ultraviolet spectrometer for remote sensing of SO2 fluxes: A new tool for volcano surveillance, J. Volcanol. Geotherm. Res., 119, 241–254, https://doi.org/10.1016/S0377-0273(02)00356-6, 2003.

General, S., Bobrowski, N., Pöhler, D., Weber, K., Fischer, C., and Platt, U.: Airborne I-DOAS measurements at Mt. Etna: BrO and OClO evolution in the plume, J of Volcanol. Geotherm. Res., 300, 175–186, https://doi.org/10.1016/j.jvolgeores.2014.05.012, 2015.

Gerlach, T. M.: Volcanic sources of tropospheric ozone-depleting trace gases, Geochem., Geophy., Geosy., 5, Q09007, https://doi.org/10.1029/2004GC000747, 2004.

Giggenbach, W. F.: Variations in the carbon, sulfur and chlorine contents of volcanic gas discharges from White Island, New Zealand, Bull. Volcanol., 39, 15–27, https://doi.org/10.1007/BF02596943, 1975.

Gliß, J., Bobrowski, N., Vogel, L., Pöhler, D., and Platt, U.: OClO and BrO observations in the volcanic plume of Mt. Etna – implications on the chemistry of chlorine and bromine species in volcanic plumes, Atmos. Chem. Phys., 15, 5659–5681, https://doi.org/10.5194/acp-15-5659-2015, 2015.

Hörmann, C., Sihler, H., Bobrowski, N., Beirle, S., Penning de Vries, M., Platt, U., and Wagner, T.: Systematic investigation of bromine monoxide in volcanic plumes from space by using the GOME-2 instrument, Atmos. Chem. Phys., 13, 4749–4781, https://doi.org/10.5194/acp-13-4749-2013, 2013.

Jourdain, L., Roberts, T. J., Pirre, M., and Josse, B.: Modeling the reactive halogen plume from Ambrym and its impact on the troposphere with the CCATT-BRAMS mesoscale model, Atmos. Chem. Phys., 16, 12099–12125, https://doi.org/10.5194/acp-16-12099-2016, 2016.

La Spina, A., Burton, M. R., Harig, R., Mure, F., Rusch, P., Jordan, M., and Caltabiano, T.: New insights into volcanic processes at Stromboli from Cerberus, a remote-controlled open-path FTIR scanner system, J. Volcanol. Geotherm. Res., 249, 66–76, https://doi.org/10.1016/j.jvolgeores.2012.09.004, 2013.

Lee, C., Kim, Y. J., Tanimoto, H., Bobrowski, N., Platt, U., Mori, T., Yamamoto, K., and Hong, C. S.: High ClO and ozone depletion observed in the plume of Sakurajima volcano, Japan, Geophys.

Res. Lett., 32, L21809, https://doi.org/10.1029/2005GL023785, 2005.

Liotta, M., Rizzo, A. L., Barnes, J. D., D'Auria, L., Martelli, M., Bobrowski, N., and Wittmer, J.: Chlorine isotope composition of volcanic rocks and gases at Stromboli volcano (Aeolian Islands, Italy): Inferences on magmatic degassing prior to 2014 eruption, J. Volcanol. Geotherm. Res., https://doi.org/10.1016/j.jvolgeores.2017.02.018, 2017.

López, T., Ushakov, S., Izbekov, P., Tassi, F., Cahill, C., Neill, O., and Werner, C.: Constraints on magma processes, subsurface conditions, and total volatile flux at Bezymianny Volcano in 2007–2010 from direct and remote volcanic gas measurements, J. Volcanol. Geotherm. Res., 263, 92–107, https://doi.org/10.1016/j.jvolgeores.2012.10.015, 2013.

Lübcke, P., Bobrowski, N., Arellano, S., Galle, B., Garzón, G., Vogel, L., and Platt, U.: BrO / SO$_2$ molar ratios from scanning DOAS measurements in the NOVAC network, Solid Earth, 5, 409–424, https://doi.org/10.5194/se-5-409-2014, 2014.

Martini, F., Tassi, F., Vaselli, O., Del Potro, R., Martinez, M., van del Laat, R., and Fernandez, E.: Geophysical, geochemical and geodetical signals of reawakening at Turrialba volcano (Costa Rica) after almost 150years of quiescence, J. Volcanol. Geotherm. Res., 198, 416–432, https://doi.org/10.1016/j.jvolgeores.2010.09.021, 2010.

Mason, E., Edmonds, M., and Turchyn, A. V.: Remobilization of crustal carbon may dominate volcanic arc emissions, Science, 357, 290–294, https://doi.org/10.1126/science.aan5049, 2017.

Mather, T. A., Pyle, D. M., Tsanev, V. I., McGonigle, A., Oppenheimer, C., and Allen, A. G.: A reassessment of current volcanic emissions from the Central American arc with specific examples from Nicaragua, J. Volcanol. Geotherm. Res., 149, 297–311, https://doi.org/10.1016/j.jvolgeores.2005.07.021, 2006.

McBirney, A. R.: The Nicaraguan volcano Masaya and its caldera, Eos Trans. AGU, 37, 83-96, https://doi.org/10.1029/TR037i001p00083, 1956.

McGonigle, A. J. S., Oppenheimer, C., Galle, B., Mather, T. A., and Pyle, D. M.: Walking traverse and scanning DOAS measurements of volcanic gas emission rates, Geophys. Res. Lett., 29, 1985, https://doi.org/10.1029/2002GL015827, 2002.

McGonigle, A. J. S., Aiuppa, A., Giudice, G., Tamburello, G., Hodson, A. J., and Gurrieri, S.: Unmanned aerial vehicle measurements of volcanic carbon dioxide fluxes, Geophys. Res. Lett., 35, L06303, https://doi.org/10.1029/2007GL032508, 2008.

Mori, T., Hashimoto, T., Terada, A., Yoshimoto, M., Kazahaya, R., Shinohara, H., and Tanaka, R.: Volcanic plume measurements using a UAV for the 2014 Mt. Ontake eruption, Earth Planet. Sp., 68, 1861, https://doi.org/10.1186/s40623-016-0418-0, 2016.

Oppenheimer, C., Tsanev, V. I., Braban, C. F., Cox, R. A., Adams, J. W., Aiuppa, A., Bobrowski, N., Delmelle, P., Barclay, J., and McGonigle, A. J.: BrO formation in volcanic plumes, Geochim. Cosmochim. Ac., 70, 2935–2941, https://doi.org/10.1016/j.gca.2006.04.001, 2006.

Palomaki, R. T., Rose, N. T., van den Bossche, M., Sherman, T. J., and de Wekker, S. F. J.: Wind Estimation in the Lower Atmosphere Using Multirotor Aircraft, J. Atmos. Ocean. Tech., 34, 1183–1191, https://doi.org/10.1175/JTECH-D-16-0177.1, 2017.

Porter, J. N., Horton, K. A., Mouginis-Mark, P. J., Lienert, B., Sharma, S. K., Lau, E., Sutton, A. J., Elias, T., and Oppenheimer, C.: Sun photometer and lidar measurements of the plume from the Hawaii Kilauea Volcano Pu'u O'o vent: Aerosol flux and SO$_2$ lifetime, Geophys. Res. Lett., 29, 30-1–30-4, https://doi.org/10.1029/2002GL014744, 2002.

Roberts, T. J., Braban, C. F., Martin, R. S., Oppenheimer, C., Adams, J. W., Cox, R. A., Jones, R. L., and Griffiths, P. T.: Modelling reactive halogen formation and ozone depletion in volcanic plumes, Chem. Geol., 263, 151–163, https://doi.org/10.1016/j.chemgeo.2008.11.012, 2009.

Roberts, T. J., Martin, R. S., and Jourdain, L.: Reactive bromine chemistry in Mount Etna's volcanic plume: The influence of total Br, high-temperature processing, aerosol loading and plume–air mixing, Atmos. Chem. Phys., 14, 11201–11219, https://doi.org/10.5194/acp-14-11201-2014, 2014.

Roberts, T. J., Saffell, J. R., Oppenheimer, C., and Lurton, T.: Electrochemical sensors applied to pollution monitoring: Measurement error and gas ratio bias at volcano plume case study, J. Volcanol. Geother. Res., 281, 85–96. https://doi.org/10.1016/j.jvolgeores.2014.02.023, 2014

Roldan, J. J., Joossen, G., Sanz, D., del Cerro, J., and Barrientos, A.: Mini-UAV based sensory system for measuring environmental variables in greenhouses, Sensors, 15, 3334–3350, https://doi.org/10.3390/s150203334, 2015.

Rüdiger, J., Bobrowski, N., Liotta, M., and Hoffmann, T.: Development and application of a sampling method for the determination of reactive halogen species in volcanic gas emissions, Anal. Bioanal. Chem., 52, 325, https://doi.org/10.1007/s00216-017-0525-1, 2017.

Shinohara, H.: A new technique to estimate volcanic gas composition: Plume measurements with a portable multisensor system, J. Volcanol. Geotherm. Res., 143, 319–333, https://doi.org/10.1016/j.jvolgeores.2004.12.004, 2005.

Symonds, R. B., Rose, W. I., Bluth, G. J. S., and Gerlach, T. M.: Volcanic-gas studies; methods, results, and applications, Rev. Mineral. Geochem., 30, 1–66, 1994.

Tamburello, G., McGonigle, A. J., Kantzas, E. P., and Aiuppa, A.: Recent advances in ground-based ultraviolet remote sensing of volcanic SO$_2$ fluxes, Ann. Geophys., 54, 199–208, https://doi.org/10.4401/ag-5179, 2011.

Theys, N., van Roozendael, M., Dils, B., Hendrick, F., Hao, N., and Mazière, M. de: First satellite detection of volcanic bromine monoxide emission after the Kasatochi eruption, Geophys. Res. Lett., 36, L03809, https://doi.org/10.1029/2008GL036552, 2009.

Villa, T. F., Gonzalez, F., Miljievic, B., Ristovski, Z. D., and Morawska, L.: An Overview of Small Unmanned Aerial Vehicles for Air Quality Measurements: Present Applications and Future Prospectives, Sensors, 16, 1072, https://doi.org/10.3390/s16071072, 2016.

von Glasow, R.: Atmospheric chemistry in volcanic plumes, P. Natl. Acad. Sci. USA, 107, 6594–6599, https://doi.org/10.1073/pnas.0913164107, 2010.

von Glasow, R., Bobrowski, N., and Kern, C.: The effects of volcanic eruptions on atmospheric chemistry, Chem. Geol., 263, 131–142, https://doi.org/10.1016/j.chemgeo.2008.08.020, 2009.

Wittmer, J., Bobrowski, N., Liotta, M., Giuffrida, G., Calabrese, S., and Platt, U.: Active alkaline traps to determine acidic-gas ratios in volcanic plumes: Sampling techniques and analytical methods, Geochem. Geophy. Geosy., 15, 2797–2820, https://doi.org/10.1002/2013GC005133, 2014.

York, D., Evensen, N. M., Martínez, M. L., and de Basabe Delgado, J.: Unified equations for the slope, intercept, and standard errors of the best straight line, Am. J. Phys., 72, 367–375, https://doi.org/10.1119/1.1632486, 2004.

Zhao, Z. and Wu, Z., Int. J. Infrared Milli, 21, 1607–1615, https://doi.org/10.1023/A:1006611609450, 2000.